Conclusions

The Infuence Function Method previously has been demonstrated to be a revolutionary new tool for the prediction of store loads in aircraft flowfields. The major limitation of the method—the difficulty and expense involved in the calibration process—has been addressed for standard missile configurations by coupling the IFM with the Interference Distributed Loads code. Significant cost reductions have been realized with no compromise in the accuracy of the IFM predictions.

References

[1] Cenko, A. and Waskiewicz, J., "Recent Improvements in Prediction Techniques for Supersonic Weapon Separation," *Journal of Aircraft*, Vol. 20, Aug. 1983, pp. 659-665.

[2] Ehlers, F. E. et al., "A Higher Order Panel Method for Linearized Supersonic Flow," NASA CR-3062, Nov. 1978.

[3] Magnus, A. E. and Epton, M. A., "PANAIR—A Computer Program for Predicting Subsonic or Supersonic Linear Potential Flows About Arbitrary Configurations Using a Higher Order Panel Method, Vol. 1, Theory Document," NASA CR-3251, 1980.

[4] Cenko, A., "PANAIR Applications to Complex Configurations," *Journal of Aircraft*, Vol. 20, Oct. 1983, pp. 887-892.

[5] Morgret, C. H., Dix, R. E., and Lijewski, L. E., "Development of Analytical and Experimental Techniques for Determining Store Airload Distributions," AIAA Paper 81-1896, 1981; *Journal of Spacecraft and Rockets*, Vol. 19, Nov.-Dec. 1982, pp. 489-495.

[6] Cenko, A., Meyer, R., Tessitore, F., Dyer, R., and Lijewski, L., "Advances in Methods for Predicting Store Aerodynamic Characteristics in Proximity to an Aircraft," AIAA Paper 83-0266, Jan. 1983.

Roll Up of Strake Leading/Trailing-Edge Vortex Sheets for Double-Delta Wings

Yin Xieyuan*

The University of Connecticut, Storrs, Connecticut

Introduction

IN recent years there has been interest in the interaction of leading/trailing-edge vortex sheets. Hummel[1] and Brennenstuhl and Hummel[2] have published a series of experimental data on the formation of leading/trailing-edge vortices for delta or double-delta wings. Kandil[3] first carried out a theoretical calculation by means of a three-dimensional nonlinear discrete vortex method. Hoeijmakers et al.[4] reported their experimental and theoretical results for delta-like wings and developed a new second-order panel method to compute double-branched spiraling vortices.

Around the same time the author attempted to simulate rolling up of leading/trailing-edge vortex sheets using a two-dimensional point vortex method in combination with a leading-edge suction analogy. The calculated results for a delta wing will be published in China. The preliminary results for a double-delta wing will be presented in this Note. In view of the inevitable instabilities in the movement of point vortices and the complex naturè of vortex sheets of double-delta wings (according to Hummel's experiments, three concentrated vortices are probably formed), the author will not employ any artificial smoothing scheme. The main purpose of this Note is to examine the capability of a simple, two-dimensional point vortex method to simulate roll up of complicated strake leading/trailing-edge vortex sheets rather than to investigate smoothing schemes. Further, the effect of the interaction of those vortex sheets on the downwash field will be considered.

Theoretical Model

This model is similar to the one used by Sacks et al.[5] According to the slender wing assumption, the original three-dimensional steady flow around a wing can be analyzed approximately by a two-dimensional time-dependent flow analogy. The separated free shear layer emanating from the leading edge of the wing is replaced by a finite number of two-dimensional point vortices. Each point vortex represents the vorticity shed from the leading edge during a time interval. Sacks' model does not rely on the assumption of conical flow.

It is convenient to use complex variables. In terms of conformal mapping, the wing section in the physical plane, $X=y+iz$, is mapped onto a circle in the transformed plane, $\zeta=\xi+i\eta$, and the resulting problem is reduced to the flow around the circle with a finite number of point vortices outside the circle. For flat-plate wing the transformation is the Joukowski transformation, $X=[\zeta+(a^2/\zeta)]$, where a is the radius of the circle. Therefore, the complex velocity potential,

$$W(\zeta)=-iV_\infty \sin\left(\zeta-\frac{a^2}{\zeta}\right) - \sum_{j=1}^{N}\frac{i\Gamma_j}{2\pi}\ln\frac{(\zeta-\zeta_j)[\zeta+(a^2/\zeta_j)]}{(\zeta+\bar{\zeta}_j)[\zeta-(a^2/\bar{\zeta}_j)]} \quad (1)$$

$$(v-iw)_k=\frac{\mathrm{d}W}{\mathrm{d}X}\bigg|_{X_k}+\frac{\mathrm{d}}{\mathrm{d}X}\left[\frac{i\Gamma_j}{2\pi}\ln(X-X_k)\right]\bigg|_{X_k} \quad (2)$$

Note that the number of point vortices, N, is variable. A new vortex shed from the leading edge is introduced into the

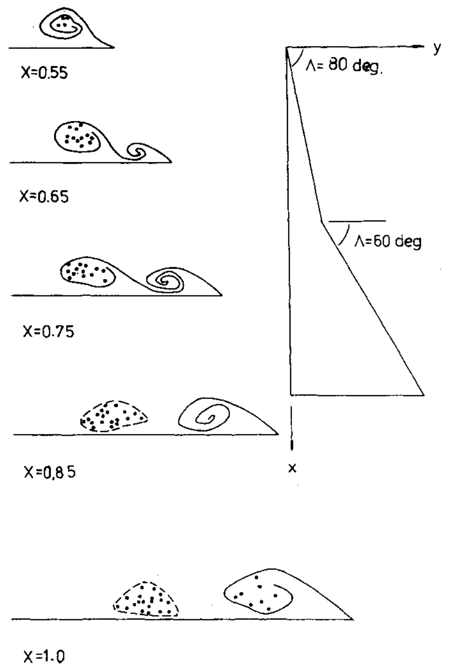

Fig. 1 Evolution of the strake leading-edge vortex sheet at $\alpha=12$ deg for Hummel's No. VI model.

Received Jan. 26, 1984; revision received May 9, 1984.

*Visiting Scientist from University of Science and Technology of China.

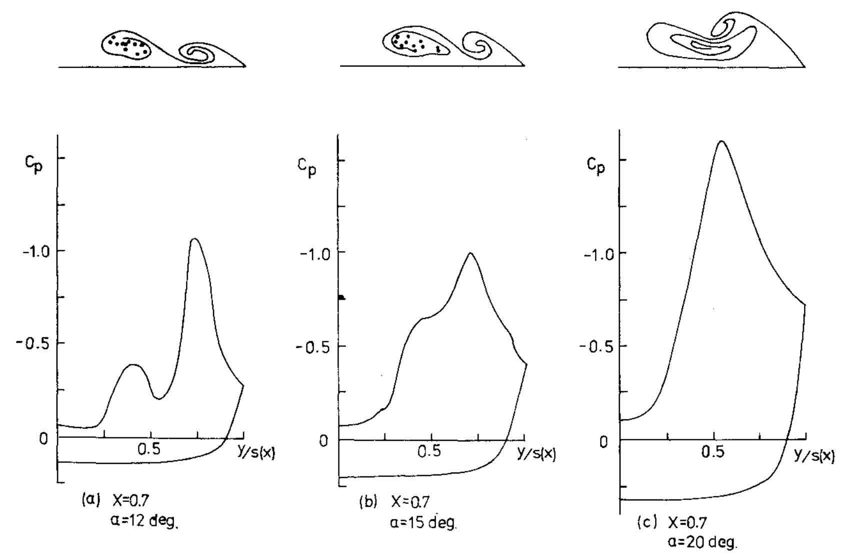

Fig. 2 Flow pattern and surface pressure distribution at $x=0.7$.

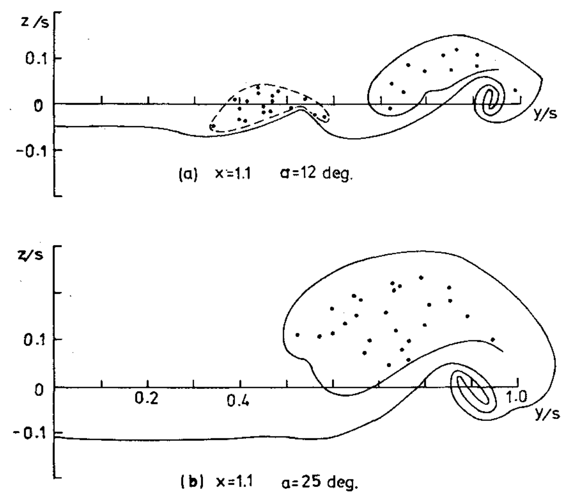

Fig. 3 Formation of trailing vortex.

flowfield at each axial station x_i. Sacks used two methods, either empirical or theoretical, to determine the new vortex strength. In this Note, the new vortex strength can be determined by using a leading-edge suction analogy as well as a vortex impulse theorem. Originally, only the overall characteristics of slender wings could be calculated by Polhamus' suction analogy. Purvis[6] suggested an analytical method that could be used to calculate the distribution of the suction along the leading edge. Then the vortex-induced lift of the front part of the axial station, x_i, is given by

$$C_{L_{\mathrm{vle}}}=E_l C_k \int_0^{\eta} (\eta_l\sqrt{1-\eta_l^2}+\sin^{-1}\eta_l)/\cos\Lambda \mathrm{d}\eta_l \tag{3}$$

The meaning of the formula can be seen from Ref. 6. On the other hand, according to the vortex impulse theorem, the vortex-induced lift is also equal to

$$C_{L_{\mathrm{vle}}}=\frac{8\pi}{S_w}\sum_{j=1}^{N-1}\frac{\Gamma_j}{2\pi V_\infty}\mathrm{Re}\left\{\zeta_j-\frac{a^2}{\zeta_j}\right\}+\frac{8\pi}{S_w}\frac{\Gamma_n}{2\pi V_\infty} \times\left(\xi_n-\frac{a^2}{\xi_n}\right) \tag{4}$$

where Γ_n and ξ_n are new vortex strength and position, respectively. Moreover, the Kutta condition must be satisfied at each axial station,

$$\sum_{j=1}^{N-1}\frac{\Gamma_j}{2\pi V_\infty}\left\{\frac{\zeta_j}{\zeta_j^2-a^2}+\frac{\bar{\zeta}_j}{\bar{\zeta}_j^2-a^2}\right\}+\frac{\Gamma_n}{2\pi V_\infty}\frac{2\xi_n}{\xi_j^2-a^2}=\sin\alpha \tag{5}$$

From Eqs. (3-5), the new vortex strength and position can be determined.

The bound vortex lines on the surface can be evaluated by

$$\gamma=-(v_u-v_l)i+(u_u-u_l)j \tag{6}$$

where the γ is vortex vector, u and v velocity components in the x and y directions, and subscripts u and l represent the upper and lower surfaces, respectively.

Downstream from the trailing edge, the trailing-edge vortex sheet must be considered along with the leading-edge vortex sheet. If the leading/trailing-edge vortex sheets are replaced by N_l and N_t point vortices, respectively, the evolution of the trailing-edge vortex sheet under the influence of the leading-edge vortex can be simulated by computing the motion of those point vortices from the trailing edge step-by-step downstream.

Numerical Results

The numerical example for Hummel's No. VI model with geometry shown in Fig. 1 has been carried out. The calculated results show that the strake vortex sheet emanating from the forward part of the leading edge upstream of the kink and the wing vortex sheet emanating from just downstream of the kink may form two separated concentrated vortices up to the trailing edge for angles of attack lower than 12 deg. Figure 1 shows the evolution of vortex sheets at subsequent stations downstream of the kink. The strake vortex sheet rolls up quite well up to $x=0.75$, after which these point vortices become very disorderly and form a group of vortex clouds.

Figure 2 shows the calculated flow pattern and surface pressure distribution at $x=0.7$ where $\alpha=12,15$, and 20 deg. At $\alpha=12$ deg, the strake and wing vortices are separated and there are two suction peaks on the upper surface beneath the strake and wing vortex cores, respectively. Although at $\alpha=15$ deg the two concentrated vortices remain distinguishable, the strake vortex moves outward, close to the wing vortex, and only one suction peak can be seen. The suction peak due to the strake vortex disappears and becomes a small protrusion on the pressure curve. At $\alpha=20$ deg the strake vortex has moved under the wing vortex and has been distorted. The shape of pressure curve is the same as that formed by one wing vortex.

The strake vortex has merged with the wing vortex at the trailing edge for $\alpha > 12$ deg. The circulation of the strake vortex is of the same sign as that of the wing vortex and is weaker than the latter. The coalesced process is related to the wing vortex strength; however, it is not clear what the coalesced condition is.

Figure 3 shows the formation of the trailing-edge concentrated vortex. The circulation of the trailing-edge vortex is of opposite sign to that of the strake and wing vortex, and the concentrated trailing-edge vortex will move outward and upward around the wing vortex. Because the strake vortex is weak, it can deform the trailing-edge vortex sheet only slightly, and not form another concentrated vortex (see Fig. 3a). In Fig. 3b, there exist one wing vortex and one trailing-edge vortex, similar to that produced by the delta wing (see Ref. 1, Fig. 12). The strake vortex has merged in this case.

The essential feature of the calculated flowfield is quite similar to that of Hummel's experiment. The pressure distribution at $x = 0.7$ is underestimated in comparison with experimental results (see Ref. 2, Fig. 9). The present method can be used qualitatively to simulate roll up of complicated vortex sheets.

References

[1] Hummel, D., "On Vortex Formation Over a Slender Wing at Large Angles of Incidence," AGARD CP-247, Jan. 1979.

[2] Brennenstuhl, U. and Hummel, D., "Untersuchungen uber die Wirbelbildung an Flugen mit Geknickten Vorderkanten," *Zeitschrift fur Flugwissenschaften und Weltraumforschung*, Vol. 5, 1981, pp. 375-381.

[3] Kandil, O. A., "Numerical Prediction of Vortex Cores from the Leading and Trailing Edge of Delta Wings," *Proceedings of the 12th Congress of the International Council of the Aeronautical Sciences*, Munich, Germany, Oct. 1980.

[4] Hoeijmakers, H. W. M. et al., "Vortex Flow Over Delta and Double-Delta Wings," *Journal of Aircraft*, Vol. 20, Sept. 1983, pp. 825-832.

[5] Sacks, A. H. et al., "A Theoretical Investigation of Slender Wing-Body Combinations Exhibiting Leading Edge Separation," NASA CR-719, March 1967.

[6] Purvis, J. W., "Analytical Prediction of Vortex Lift," *Journal of Aircraft*, Vol. 18, April 1981, pp. 225-230.

Determination of Subcritical Damping in CF-5 Flight Flutter Tests

B. H. K. Lee*
National Aeronautical Establishment,
National Research Council Canada, Ottawa, Canada

Introduction

ONE of the fundamental tasks when investigating the flutter characteristics of an aircraft is the determination of subcritical damping values of the various modes of vibration of the aircraft structure as functions of the flight velocity and altitude. There are various methods commonly used to excite the airframe in flight flutter tests. The use of stick raps has been adopted by the Canadian Forces in their flutter clearance program of CF-5 aircraft with external stores configurations. Symmetric and antisymmetric modes of the aircraft wing can be excited rather simply by the application of elevator or aileron pulses.

Flight Testing of the CF-5

The test aircraft was instrumented with eight accelerometers. Four were positioned at the front and rear of the tip tanks and these were the primary ones used for flutter investigation. The remaining four accelerometers were located at the nose of the wing-mounted stores and served mainly to provide vibration data of the stores. Reference 1 gives a detailed description of the test facilities and procedures. In this Note, some results for the LAU-5003/A rocket launchers are presented. The configuration for the flight test consisted of LAU-5003/A rocket launchers carrying nineteen C14 rockets with MK 1 warheads at the outboard pylons and eleven C14 rockets with MK 1 warheads at the inboard pylons. The launchers were equipped with nose cones. The aircraft carried a 150 US gallon centerline tank and two tip tanks.

All tests were performed at an altitude of approximately 7000 ft above sea level. Lateral and longitudinal stick raps were initiated by the pilot, and the response was allowed to decay for a sufficiently long time to permit on-line analysis. Based on analytical predictions and on previous experience, four structural modes were of primary interest in the LAU-5003/A flutter tests. They were the symmetric and antisymmetric wing bending and torsional modes. To improve identification of individual modes, power spectral densities were obtained from four different linear combinations of the four accelerometer signals.[1] Each linear combination was aimed at enhancing the power spectrum of one of the four modes of interest, and from the power spectrum, modal frequencies and damping values were deduced.

Determination of Damping

In transient testing using stick pulses, the excitation forces generated are frequently represented by an impulse function. The damping g is obtained from the equation

$$g = \Delta f / f_{\max} \tag{1}$$

where $f_{\max}$ is the frequency at the peak of the response power spectral density curve and Δf corresponds to the width of the

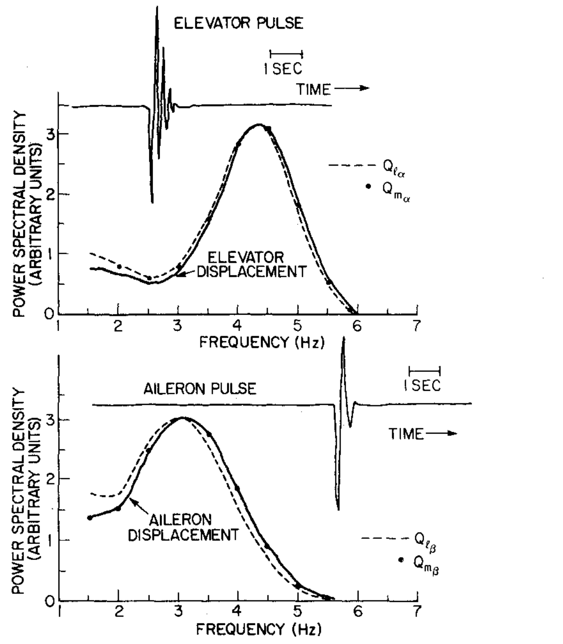

Fig. 1 Time history and power spectral density for elevator and aileron displacements.

Received Jan. 23, 1984; revision received June 22, 1984.

*Senior Research Officer, High Speed Aerodynamics Laboratory. Member AIAA.